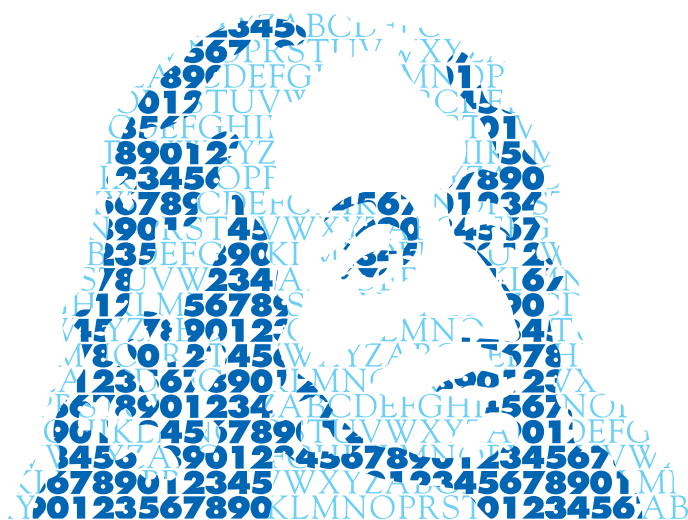


# ANNALES MATHÉMATIQUES



## BLAISE PASCAL

ENRIQUE FERNÁNDEZ-CARA,  
THIERRY HORSIN & HENRY KASUMBA

**Some inverse and control problems for fluids**

Volume 20, n° 1 (2013), p. 101-138.

[http://ambp.cedram.org/item?id=AMBP\\_2013\\_\\_20\\_1\\_101\\_0](http://ambp.cedram.org/item?id=AMBP_2013__20_1_101_0)

© Annales mathématiques Blaise Pascal, 2013, tous droits réservés.

L'accès aux articles de la revue « Annales mathématiques Blaise Pascal » (<http://ambp.cedram.org/>), implique l'accord avec les conditions générales d'utilisation (<http://ambp.cedram.org/legal/>). Toute utilisation commerciale ou impression systématique est constitutive d'une infraction pénale. Toute copie ou impression de ce fichier doit contenir la présente mention de copyright.

*Publication éditée par le laboratoire de mathématiques  
de l'université Blaise-Pascal, UMR 6620 du CNRS  
Clermont-Ferrand — France*

**cedram**

Article mis en ligne dans le cadre du  
Centre de diffusion des revues académiques de mathématiques  
<http://www.cedram.org/>

# Some inverse and control problems for fluids

ENRIQUE FERNÁNDEZ-CARA  
THIERRY HORSIN  
HENRY KASUMBA

## Abstract

This paper deals with some inverse and control problems for the Navier-Stokes and related systems. We will focus on some particular aspects that have recently led to interesting (theoretical and numerical) results: geometric inverse problems, Eulerian and Lagrangian controllability and vortex reduction oriented to shape optimization.

## *Quelques problèmes inverses et de contrôles pour les fluides*

### Résumé

Ce papier discute quelques problèmes inverses et de contrôle pour des systèmes de type Navier-Stokes. On insiste sur quelques aspects de nature à la fois théorique et numérique ayant menés récemment à des résultats nouveaux : Problèmes inverses géométriques, Contrôlabilité Eulérienne et Lagrangienne, Réduction de tourbillons par optimisation de forme, etc.

## CONTENTS

1. Introduction. Motivation and general description	102
2. Some recent results and open questions concerning the control of fluids	103
2.1. An inverse problem	103
2.2. Controllability: first results	107
2.3. Numerical controllability of the Navier-Stokes equations	110
3. Lagrangian controllability of some fluid models	115
3.1. The Lagrangian controllability	116
3.2. The main result in dimension 2	117

---

*Keywords:* Navier-Stokes equations, Euler equations, inverse problems, exact and approximate controllability, Lagrangian controllability, vortex reduction, shape optimization.

*Math. classification:* 35R30, 76B75, 76D55.

3.3.	The main result in dimension 3	118
3.4.	A cornerstone of the proofs	119
3.5.	Towards numerics	120
3.6.	Extension to other models	121
4.	Vortex control of instationary channel flows using translation invariant cost functionals	121
4.1.	Setting of the problem	123
4.1.1.	The state equation	123
4.1.2.	The optimization problems	123
4.2.	Sensitivity analysis	124
4.3.	Numerical algorithm and examples	127
4.3.1.	Test case 1: flow in a channel with a bump	127
4.3.2.	Test case 2: flow in a channel with an obstacle	130
	References	132

## 1. Introduction. Motivation and general description

The control and the parameter identification of fluids have been the origin of a lot of interesting work the last decades.

We can mention many challenging motivations of practical interest: the stabilization of turbulent flows, the control and transport of contamination, the optimal design of aerodynamic profiles, weather forecasting, etc.

The main purposes of this paper are the following:

- To recall some still unsolved control and inverse problems for the Navier-Stokes equations and related systems.
- To report on the progress that several researchers have recently made in this setting.

Of course, it is impossible to cover a significative part of the subject, but we can indicate a few questions leading to nontrivial mathematical and numerical problems. For many other questions and results, the reader is referred for instance to the general references [28, 29, 34, 35, 37, 38]; see also [5, 14, 49].

The paper is organized as follows.

In Section 2, we first consider some geometric inverse problems concerning the identification of the shape of a body in a viscous fluid; we recall

some results that provide uniqueness and partial reconstruction from local boundary observation. We also consider some (Eulerian) controllability problems and we recall recent theoretical and numerical results.

In Section 3, we deal with Lagrangian controllability. Specific results concerning the Euler equations will be given, describing how to settle the main definition of this notion, as well as a comparison with the controllability in Eulerian descriptions. Some works in progress on numerics and other fluid models will be also discussed.

Finally, in Section 4, the use of translation invariant cost functionals for the reduction of vortices is investigated in the context of shape optimization of fluid flow domains. Analytical expressions for the shape design sensitivity involving various functionals are derived. Instationary channel flow problems with a bump and an obstacle as possible control boundaries are taken as test examples. Numerical results are provided for relatively low Reynolds numbers and some conclusions are obtained.

## 2. Some recent results and open questions concerning the control of fluids

This Section is devoted to motivate the subject through several nontrivial problems. In particular, an inverse problem concerning the shape identification of an immersed body will be considered. Also, the approximate and null controllability problems for the Navier-Stokes equations with distributed or boundary controls, locally supported in space, will be recalled.

### 2.1. An inverse problem

In general terms, the formulation of an inverse problem has the following structure:

- It is assumed that a system describes the phenomena under study. In this system, the “natural” data are collected in two sets  $\mathcal{D}_0$  and  $\mathcal{D}_1$  and the solution  $\mathcal{S}$  yields an observation  $\mathcal{I}$ .
- The data  $\mathcal{D}_0$  are known. Contrarily, the data  $\mathcal{D}_1$  are unknown but we have access to the additional information  $\mathcal{I}$ . The goal is then to recover  $\mathcal{D}_1$  from  $\mathcal{D}_0$  and  $\mathcal{I}$ .

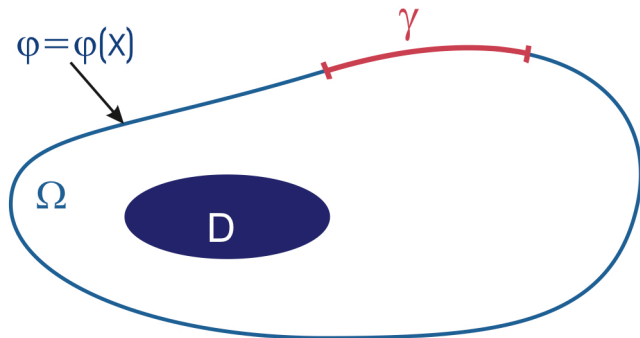


FIGURE 2.1. The sets  $\Omega$  and  $D$ .

Among all the questions that can be considered for inverse problems of this kind, let us mention the following:

- (1) Uniqueness: Is it true or not that  $\mathcal{D}_0 = \mathcal{D}'_0$  and  $\mathcal{I} = \mathcal{I}'$  implies  $\mathcal{D}_1 = \mathcal{D}'_1$ ?
- (2) Stability: Is it possible to “estimate” the distance or deviation from  $\mathcal{D}_1$  to  $\mathcal{D}'_1$  in terms of the distance from  $\mathcal{D}_0$  to  $\mathcal{D}'_0$  and the distance from  $\mathcal{I}$  to  $\mathcal{I}'$ ?
- (3) Reconstruction: Can  $\mathcal{D}_1$  be (exactly or approximately) computed from  $\mathcal{D}_0$  and  $\mathcal{I}$ ?

The reader can find information on the state of the art of this interesting area for instance in [42, 47, 54] and the references therein.

The inverse problem in this Section is the following. Assume that  $N = 2$  or  $N = 3$  and a regular bounded connected open set  $\Omega \subset \mathbb{R}^N$ , a non-zero function  $\varphi$  satisfying

$$\varphi \in C^1(\partial\Omega)^N, \quad \int_{\partial\Omega} \varphi \cdot n \, d\Gamma = 0,$$

a non-empty open set  $\gamma \subset \partial\Omega$  and a function  $\alpha = \alpha(x)$  on  $\gamma$  are given; see Figure 2.1. Then, the goal is to find a non-empty simply connected

open set  $D \subset\subset \Omega$  such the stationary Navier-Stokes system

$$\begin{aligned}
 -\nu\Delta u + (u \cdot \nabla)u + \nabla p &= 0, & x \in \Omega \setminus D \\
 \nabla \cdot u &= 0, & x \in \Omega \setminus D \\
 u &= 0, & x \in \partial D \\
 u &= \varphi, & x \in \partial\Omega
 \end{aligned} \tag{2.1}$$

possesses a solution  $(u, p)$  satisfying

$$\sigma(u, p) \cdot n := \left(-p\text{Id.} + \nu(\nabla u + \nabla u^T)\right) \cdot n = \alpha, \quad x \in \gamma.$$

In other words, we try to find the shape of a body immersed in a viscous newtonian fluid using as data the velocity trace  $u|_{\partial\Omega}$  and the normal stresses  $\sigma(u, p) \cdot n$  on  $\gamma$ .

Geometric inverse problems of this kind have been analyzed by several authors; see for instance [3, 1, 2, 56]. In particular, the following results, concerning uniqueness and partial reconstruction, have been proven in [19]:

**Theorem 2.1.** *Let  $D^1$  and  $D^2$  be two simply connected open sets satisfying*

$$D^i \subset\subset \Omega, \quad \partial D^i \in W^{2,\infty},$$

*let  $(u^i, p^i)$  be the solution to (2.1) for  $D = D^i$  and let us set  $\alpha^i = \sigma(u^i, p^i) \cdot n|_{\gamma}$  for  $i = 1, 2$ . Assume that*

$$\alpha^1 = \alpha^2 \quad \text{on } \gamma. \tag{2.2}$$

*Then  $D^1 = D^2$ .*

The proof of this result follows an argument that can be found for other problems for instance in [3, 9] and relies on a unique continuation property of the linearized Navier-Stokes system. More precisely, let  $D^1$  and  $D^2$  be given and let us assume that (2.2) holds. Let us consider the open sets  $D^1 \cup D^2 \in \mathcal{D}$  and  $\mathcal{O}^0 = \Omega \setminus \overline{D^1 \cup D^2}$ , let  $\mathcal{O}$  be the unique connected component of  $\mathcal{O}^0$  whose boundary contains  $\partial\Omega$  and let us introduce

$$v = u^1 - u^2 \quad \text{and} \quad \pi = p^1 - p^2.$$

Then,  $(v, \pi) \in H^1(\mathcal{O})^N \times L^2(\mathcal{O})$  and, from the already mentioned unique continuation result, one has

$$v = 0 \quad \text{in } \mathcal{O},$$

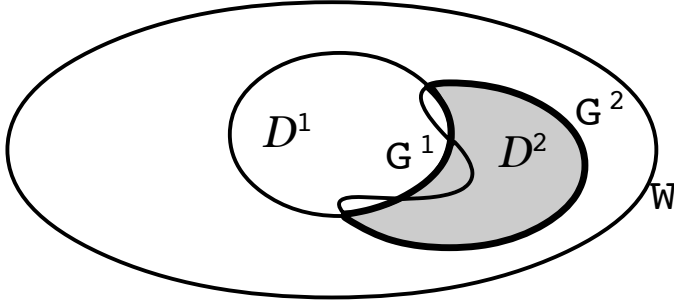


FIGURE 2.2. The dashed set is  $D^3 \setminus \overline{D^1}$ .

that is to say,

$$u^1 = u^2 \text{ in } \mathcal{O}.$$

For instance, let us assume that  $D^2 \setminus \overline{D^1} \neq \emptyset$  and let us set  $D^3 = D^2 \cup ((\Omega \setminus \overline{D^1}) \cap (\Omega \setminus \overline{\mathcal{O}}))$ . By hypothesis,  $D^3 \setminus \overline{D^1}$  is nonempty. Moreover,  $\partial(D^3 \setminus \overline{D^1}) = \Gamma^1 \cup \Gamma^2$ , where  $\Gamma^1 = \partial(D^3 \setminus \overline{D^1}) \cap \partial D^1$  and  $\Gamma^2 = \partial(D^3 \setminus \overline{D^1}) \cap \partial D^2$  (see Figure 2.2).

The couple  $(u^1, p^1)$  solves the homogeneous Navier-Stokes system in  $D^3 \setminus \overline{D^1}$  with zero data on the boundary. Of course, this implies  $u^1 = 0$  in  $D^3 \setminus \overline{D^1}$  and also  $u^1 \equiv 0$ , which is impossible because  $u^1 = \varphi$  on  $\partial\Omega$ . Therefore,  $D^2 \setminus \overline{D^1}$  is the empty set.

We can prove in the same way that the set  $D^1 \setminus \overline{D^2}$  is empty. Therefore,  $D^1 = D^2$ .

**Theorem 2.2.** *Let  $D^i$ ,  $(u^i, p^i)$  and  $\alpha^i = \sigma(u^i, p^i) \cdot n$  be as in Theorem 2.1 and assume that*

$$D^2 = D^1 + m := \{x + m(x) : x \in D^1\}$$

*with  $m = \lambda n + m'$  on  $\partial D^1$ ,  $\lambda \in \mathbb{R}$ ,  $m' \in W^{2,\infty}(\mathbb{R}^N; \mathbb{R}^N)$  and  $m' \cdot n = 0$  ( $n = n(x)$  is the unit normal on  $D^1$ ). Let  $\overline{\psi}$  satisfy*

$$\overline{\psi} \in C^2(\overline{\gamma})^N, \quad \int_{\gamma} \overline{\psi} \cdot n \, d\Gamma = 0,$$

let us denote by  $(\psi, \pi)$  the solution to the adjoint system

$$\begin{aligned} -\nu\Delta\psi - (\nabla u^1)^t\psi - (u^1 \cdot \nabla)\psi + \nabla\pi &= 0, & x \in \Omega \setminus \overline{D^1} \\ \nabla \cdot \psi &= 0, & x \in \Omega \setminus \overline{D^1} \\ \psi &= \overline{\psi} 1_\gamma, & x \in \partial\Omega \\ \psi &= 0, & x \in \partial D^1 \end{aligned}$$

and let us assume that

$$\int_{\partial D^1} \frac{\partial u^1}{\partial n} \cdot \frac{\partial \psi}{\partial n} d\Gamma \neq 0.$$

Then there exists  $\varepsilon > 0$  such that, if  $\|m\|_{W^{2,\infty}} \leq \varepsilon$ , one has

$$\lambda = -\frac{\langle \alpha^2 - \alpha^1, \overline{\psi} 1_\gamma \rangle}{\nu \int_{\partial D^1} \frac{\partial u^1}{\partial n} \cdot \frac{\partial \psi}{\partial n} d\Gamma} + o(\|m\|_{W^{2,\infty}}). \quad (2.3)$$

The proof relies on appropriate domain variation techniques, see [6]. Thus, for small  $\|m\|_{W^{2,\infty}}$ , it is possible to expand up to first order terms the quantity  $\langle \alpha^2, \overline{\psi} 1_\gamma \rangle$  in terms of  $\langle \alpha^1, \overline{\psi} 1_\gamma \rangle$  and the “derivative” of the mapping  $m \mapsto \langle \sigma(u, p) \cdot n, \overline{\psi} 1_\gamma \rangle$ . After some computations, this yields (2.3).

We refer to [2] and [18] for other similar results. To our knowledge, the numerical solution of the inverse problem considered in this Section via efficient methods remains open.

## 2.2. Controllability: first results

In the formulation of a controllability problem, we usually find the following elements:

- A time-dependent system that describes the considered phenomena. In this system, one or several data can be chosen freely in a set of constraints; these are the controls. The solution to the system is called the (time-dependent) state.
- A set of desired final states, i.e., a set where we would like to have the solution at the final time.

Of course, the goal is to find admissible controls (that is, controls in the constraint set) such that an associated solution evolves to a desired state.

Let us be more precise and let us present some first (Eulerian) controllability problems and results.

Let  $\Omega$  be as in Section 2.1 and let us introduce the space

$$H = \{v \in L^2(\Omega)^N : \nabla \cdot v = 0 \text{ in } \Omega, \quad v \cdot n = 0 \text{ on } \partial\Omega\}.$$

Assume that the phenomena under study are modelled by the Navier-Stokes system

$$\begin{aligned} u_t + (u \cdot \nabla)u - \nu \Delta u + \nabla p &= v 1_\omega, & (x, t) \in Q_T \\ \nabla \cdot u &= 0, & (x, t) \in Q_T \\ u &= 0, & (x, t) \in \Sigma_T \\ u(x, 0) &= u_0(x), & x \in \partial\Omega \end{aligned} \tag{2.4}$$

where  $T > 0$ ,  $Q_T = \Omega \times (0, T)$ ,  $\Sigma_T = \partial\Omega \times (0, T)$ ,  $\omega \subset \Omega$  is a (small) non-empty open subset,  $v \in L^2(\omega \times (0, T))^N$  and  $u_0 \in H$ .

In (2.4),  $v$  is the control and  $u$  is the state. It will be said that (2.4) is *approximately controllable* at time  $T$  if, for any  $u_0, u_T \in H$  and any  $\varepsilon > 0$ , there exists  $v \in L^2(\omega \times (0, T))^N$  and an associated solution  $u \in C_w^0([0, T]; H)$  such that

$$\|u(\cdot, T) - u_T\|_{L^2} \leq \varepsilon.$$

It will be said that (2.4) is *null-controllable* at time  $T$  if, for any  $u_0 \in H$ , there exists a control  $v \in L^2(\omega \times (0, T))^N$  and an associated solution  $u \in C_w^0([0, T]; H)$  such that

$$u(x, T) = 0, \quad x \in \Omega. \tag{2.5}$$

At present, the approximate and null controllability of (2.4) are open questions. However, some partial results are known:

- For Stokes or Stokes-like systems, approximate and null controllability hold for all  $\omega$  and  $T$ ; see [22, 23].
- For Navier-Stokes systems like (2.4) completed with other boundary conditions, controllability results can also be obtained; see for instance [15, 30, 17].
- If we keep Dirichlet boundary conditions in (2.4), we can establish local results. For instance, this means that there exists  $\varepsilon > 0$  such that, for any  $y_0 \in H$  with  $\|y_0\|_{L^2} \leq \varepsilon$ , there exist controls and associated states satisfying (2.5). For results of this kind, see [41, 23, 24].

Let us now recall the main result in [23]. It deals with the local exact controllability to the bounded trajectories and, in particular, implies local null controllability for (2.4).

**Theorem 2.3.** *Let  $(\bar{u}, \bar{p})$  be a solution to (2.4) corresponding to the initial state  $\bar{u}_0 \in L^{2N-2}(\Omega)^N \cap H$  and the control  $\bar{v} = 0$ . Assume that  $\bar{u} \in L^\infty(\Omega \times (0, T))^N$ . There exists  $\varepsilon > 0$  with the following property: for any initial  $u_0$  satisfying  $\|\bar{u}_0 - u_0\|_{L^{2N-2}} \leq \varepsilon$ , we can find controls  $v \in L^2(\omega \times (0, T))^N$  and associated states  $(u, p)$  such that*

$$u(x, T) = \bar{u}(x, T), \quad x \in \Omega. \quad (2.6)$$

For the proof, we first rewrite (2.6) as a null controllability property for a modified Navier-Stokes system. Thus, we introduce  $y := u - \bar{u}$ , we notice that

$$\begin{aligned} y_t + ((\bar{u} + y) \cdot \nabla)y + (y \cdot \nabla)\bar{u} - \nu \Delta y + \nabla \pi &= v \mathbf{1}_\omega, & (x, t) \in Q_T \\ \nabla \cdot y &= 0, & (x, t) \in Q_T \\ y &= 0, & (x, t) \in \Sigma_T \\ y(x, 0) &= y_0(x) := u_0(x) - \bar{u}_0(x), & x \in \partial\Omega \end{aligned} \quad (2.7)$$

and we search for controls  $v$  such that

$$y(x, T) = 0, \quad x \in \Omega.$$

Then, we apply an appropriate *inverse mapping theorem* and we see that the task is reduced to prove the null controllability of the Stokes-like system

$$\begin{aligned} y_t + (\bar{u} \cdot \nabla)y + (y \cdot \nabla)\bar{u} - \nu \Delta y + \nabla \pi &= v \mathbf{1}_\omega, & (x, t) \in Q_T \\ \nabla \cdot y &= 0, & (x, t) \in Q_T \\ y &= 0, & (x, t) \in \Sigma_T \\ y(x, 0) &= y_0(x), & x \in \partial\Omega \end{aligned} \quad (2.8)$$

Finally, we see that the latter is implied by the global Carleman estimates deduced in [23] for the associated adjoint problem. More precisely, we consider the solutions to the systems

$$\begin{aligned} -\varphi_t - (D\varphi) \bar{u} - \nu \Delta \varphi + \nabla q &= g(x, t), & (x, t) \in Q_T \\ \nabla \cdot \varphi &= 0, & (x, t) \in Q_T \\ \varphi &= 0, & (x, t) \in \Sigma_T \\ \varphi(x, T) &= \varphi_T(x), & x \in \partial\Omega \end{aligned} \quad (2.9)$$

where  $g \in L^2(Q_T)^N$  and  $\varphi_T \in H$  and we prove that there exist appropriate weights  $\rho, \rho_*, \rho_0, \rho_1, \dots$  (that blow up as  $t \rightarrow T^-$ ) and a constant  $C$  such that

$$\begin{aligned} & \iint_{Q_T} \left( \rho_2^{-2} (|\varphi_t|^2 + |\Delta\varphi|^2) + \rho_1^{-2} |\nabla\varphi|^2 + \rho_0^{-2} |\varphi|^2 \right) dx dt \\ & \leq C \left( \iint_{Q_T} \rho^{-2} |g|^2 dx dt + \iint_{\omega \times (0, T)} \rho_*^{-2} |\varphi|^2 dx dt \right) \end{aligned} \quad (2.10)$$

Then, we deduce the null controllability of (2.9) from (2.10) using a classical duality argument.

Results of this kind can be proven for other more complex systems. For instance, the following problem is considered in [24, 36]:

$$\begin{aligned} u_t + (u \cdot \nabla)u - \nu\Delta u + \nabla p &= \theta k + v1_\omega, & (x, t) \in Q_T \\ \nabla \cdot u &= 0, & (x, t) \in Q_T \\ \theta_t + u \cdot \nabla\theta - \kappa\Delta\theta &= w1_\omega, & (x, t) \in Q_T \\ u = 0, \theta = 0, & & (x, t) \in \Sigma_T \\ u(x, 0) = u_0(x), \theta(x, 0) &= \theta_0(x), & x \in \partial\Omega \end{aligned}$$

where  $k \in \mathbb{R}^N$ ,  $\kappa > 0$ ,  $v \in L^2(\omega \times (0, T))^N$  and  $w \in L^2(\omega \times (0, T))$  are the controls,  $u_0 \in H$  and  $\theta_0 \in L^2(\Omega)$ . This is the so called Boussinesq system, a common model for the flow of a viscous newtonian fluid where heat effects are important, see for instance [11, 27].

### 2.3. Numerical controllability of the Navier-Stokes equations

The numerical analysis of controllability problems for PDEs such as those above is very involved. The main reason is that the systems are parabolic and, consequently, the solutions are regularized at positive time, a property that is very complicated to reproduce at the numerical level.

Up to now, the approximation of the null control of minimal  $L^2$  norm has focused most of the attention. The first contribution was made by Carthel, Glowinski and Lions in [10], in the context of the linear heat equation, where duality arguments were introduced. But the resulting problem is numerically ill-posed; see [46, 52, 53] and [7], where the degree of ill-posedness is investigated in the boundary situation.

In [50], in the context of approximate controllability, a relaxed observability inequality is given for general semi-discrete (in space) schemes,

with the parameter  $\varepsilon$  of the order of  $\Delta x$ . The work [8] extends the results in [50] to the fully discrete situation and proves the convergence towards a semi-discrete control, as the time step  $\Delta t$  tends to zero. Let us also mention [20], where the authors prove that any controllable parabolic equation, be it discrete or continuous in space, is null-controllable after time discretization through the application of an appropriate filtering of the high frequencies. As far as we know, a strong convergence result in the framework of dual method is still missing.

In some recent papers, the first author and A. Münch have applied different techniques, inspired by the results of A.V. Fursikov and O. Yu. Imanuvilov [31], to the computation of “good” numerical approximations to null controls of linear and nonlinear parabolic PDEs; see [26, 25]. These techniques have been extended in [13], where linear problems of the Stokes kind and also Navier-Stokes systems are considered.

The idea is the following.

• First, assume that  $\bar{y}$  is given in  $C^0([0, T]; H) \cap L^\infty(Q_T)^N$  and we want to compute  $v$  such that the solution to

$$\begin{aligned} y_t + ((\bar{u} + \bar{y}) \cdot \nabla) y + (y \cdot \nabla) \bar{u} - \nu \Delta y + \nabla \pi &= v \mathbf{1}_\omega, & (x, t) \in Q_T \\ \nabla \cdot y &= 0, & (x, t) \in Q_T \\ y &= 0, & (x, t) \in \Sigma_T \\ y(x, 0) &= y_0(x), & x \in \partial\Omega \end{aligned} \quad (2.11)$$

satisfies

$$y(x, T) = 0, \quad x \in \Omega. \quad (2.12)$$

Then, we introduce the following extremal problem:

$$\begin{aligned} \text{Minimize } J(y, v) &= \frac{1}{2} \iint_{Q_T} \rho^2 |y|^2 dx dt + \frac{1}{2} \iint_{Q_T} \rho_*^2 |v|^2 dx dt \\ \text{Subject to } (y, v) &\in \mathcal{C}(y_0; T), \end{aligned} \quad (2.13)$$

where

$$\mathcal{C}(y_0; T) = \{ (y, v) : v \in L^2(\omega \times (0, T))^N, (y, v) \text{ satisfies (2.11), (2.12)} \}.$$

Obviously, a solution  $(y, v)$  to (2.13) provides at once a “good” (in some sense optimal) solution to the null controllability problem for (2.8).

It can be seen that (2.13) possesses exactly one solution, given by

$$y = \rho^{-2}(L^* w + \nabla \sigma), \quad v = -\rho_0^{-2} w|_{\omega \times (0, T)},$$

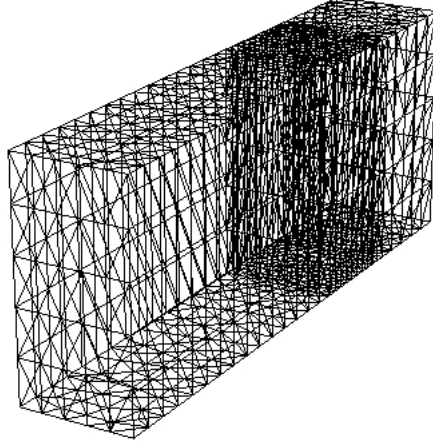


FIGURE 2.3. The domain  $Q_T$  and the mesh. The  $x$ ,  $y$  and  $t$  axis are respectively directed from left to right, from right to left and upwards. Number of vertices: 1830, number of elements: 7830, number of degrees of freedom: 12485.

where  $(w, \sigma)$  is the unique solution to the fourth-order variational equality

$$\begin{aligned} & \iint_{Q_T} \left( \rho^{-2} (L^* w + \nabla \sigma) \cdot (L^* w' + \nabla \sigma') + 1_\omega \rho_0^{-2} w \cdot w' \right) dx dt \\ & = \int_{\Omega} y_0(x) \cdot w'(x, 0) dx \quad \forall (w', \sigma') \in \Phi; (w, \sigma) \in \Phi \end{aligned} \quad (2.14)$$

and we have introduced the notation  $L^* w := -w_t - \nu \Delta w$ .

Here,  $\Phi$  is the Hilbert space defined as follows. First, we introduce the linear space

$$\Phi_0 := \{ (w, \sigma) \in C^2(\overline{Q_T})^{N+1} : \nabla \cdot w \equiv 0, w = 0 \text{ on } \Sigma_T \}.$$

Then, we notice that the bilinear form in the left hand side of (2.14) is a scalar product in  $\Phi_0$ . Finally, we define  $\Phi$  as the completion of  $\Phi_0$  for this scalar product. Thanks to the choice of the weights and, more precisely,

thanks to (2.10), the right hand side in (2.14) provides a continuous linear form on  $\Phi$  and this variational equality is well posed.

Unfortunately, if  $(w, \sigma) \in \Phi$ , then  $L^*w + \nabla\sigma$  must be locally square integrable in  $Q_T$ . In practice, we see that, for the definition of a finite-dimensional subspace of  $\Phi$ , we have to work with functions with second-order spatial derivatives in  $L^2_{\text{loc}}(Q_T)$  and this is a (maybe too) strong requirement. This argument shows that it can be a good idea to relax the constraints

$$y - \rho^{-2}(L^*w + \nabla\sigma) = 0 \quad \text{and} \quad \nabla \cdot w = 0$$

by introducing appropriate multipliers, to rewrite (2.14) as a mixed variational problem of the form

$$\begin{aligned} a((y, w, \sigma), (y', w', \sigma')) + b((y', w', \sigma'), (\lambda, \mu)) &= \int_{\Omega} y_0(x) \cdot w'(x, 0) dx \\ b((y, w, \sigma), (\lambda', \mu')) &= 0 \\ \forall (y', w', \sigma', \lambda', \mu') \in X; (y, w, \sigma, \lambda, \mu) \in X \end{aligned}$$

(with appropriate definitions of  $a(\cdot, \cdot)$ ,  $b(\cdot, \cdot)$  and  $X$ ) and, then, consider finite-dimensional approximations.

Notice that, by integrating by parts with respect to the spatial variables in  $b((y', w', \sigma'), (\lambda, \mu))$  and  $b((y, w, \sigma), (\lambda', \mu'))$ , the second-order derivatives disappear. Accordingly, with the help of a standard triangulation of  $\Omega$  and the associated usual  $P_\ell$ -Lagrange finite element spaces, we obtain a relatively reasonable linear system.

- Secondly, we can apply a fixed-point algorithm to solve the null controllability problem for (2.7). Obviously, this furnishes a numerical solution to the problem of exact controllability to the trajectories: how can we compute a control that drives a solution to (2.4) exactly to  $\bar{u}(\cdot, T)$  at time  $T$ .

Indeed, to any  $\bar{y} \in L^\infty(Q_T)^N$  we can associate the solution  $(y, v)$  to the corresponding problem (2.13) and then the state  $y$ . If  $y_0$  is sufficiently small (that is, if  $u_0$  is sufficiently close to  $\bar{u}_0$ ), it can be expected that the related iterates converge.

In order to illustrate the situation, let us present the results of an experiment. We solve numerically the exact controllability problem for (2.4)

with  $N = 2$ ,  $\Omega = (0, 5) \times (0, 1)$ ,  $T = 2$ ,  $\nu = 1$ ,  $\omega = (1, 2) \times (0, 1)$ ,

$$y_0 = \nabla \times \psi_0, \quad \psi_0(x_1, x_2) \equiv 0.1x_1^2x_2^2(5 - x_1)^2(1 - x_2)^2$$

and

$$\bar{u}(x_1, x_2, t) \equiv (4x_2(1 - x_2), 0)$$

for all  $t$ , i.e., the Poisseuille flow.

The space-time domain and the mesh are displayed in Figure 2.3. We have used the previous mixed formulation, relying on the standard  $P_2$ -Lagrange finite element spaces.

The resulting system has a considerable size. Furthermore, it is readily seen after inspection that the coefficient matrix corresponding to the bilinear form  $a(\cdot, \cdot)$  can be difficult to invert, since it is only semidefinite positive in  $w$ . Accordingly, the system has been solved with the Arrow-Hurwicz method [4], that provides very acceptable results, better than a direct solver. The iterates have been stopped when the relative error of two consecutive iterates is less than  $10^{-5}$ . The computed control and state are shown in Figures 2.4–2.5.

The computations have been performed with the FreeFem++ package, see <http://www.freefem.org/ff++>. More information, a detailed analysis and other similar numerical experiments will appear in [13].

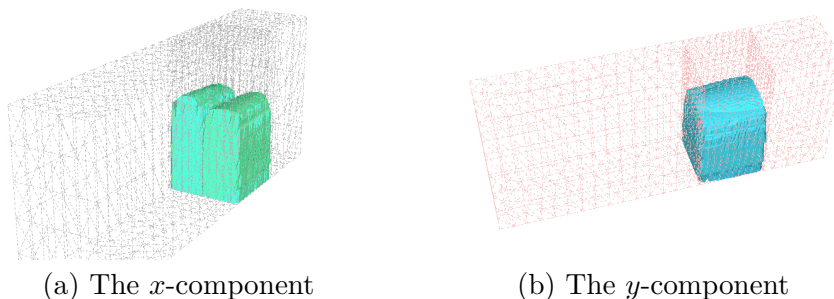


FIGURE 2.4. 3D views of the computed control components.

This method can be extended to cover other controllable systems for which appropriate Carleman estimates are available, including hyperbolic models, see [12]. It is also possible to adapt the arguments to the boundary controllability framework.

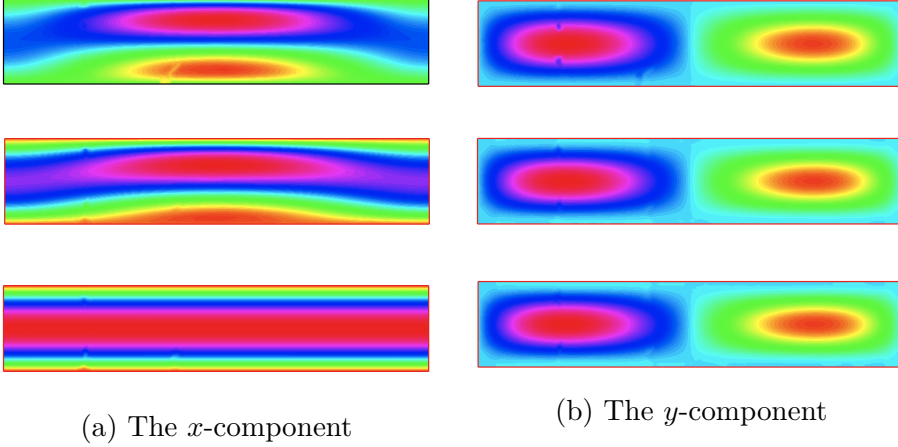


FIGURE 2.5. The computed states for  $t = 0, 0.8, 1.6$ . The minima and maxima are the following:  $-0.98$  and  $2.38$ ,  $-0.09$  and  $1.33$  and  $-0.03$  and  $1.03$  for the  $x$ -component;  $-0.32$  and  $0.32$ ,  $-0.09$  and  $0.09$  and  $-10^{-4}$  and  $10^{-4}$  for the  $y$ -component. This shows that the state is driven to Poiseuille flow by the action of the computed control.

### 3. Lagrangian controllability of some fluid models

How to describe the flow of a fluid has been a challenging question along history for several reasons. A relevant aspect to be taken into account is the ability to distinguish the motion of the fluid particles while observing a fluid flooding with different colored components. Another requirement is motivated by the interest of fishermen observing (ideally motionless) floats and deducing the motion of the particles from the generated wake. These considerations were already in the core of the works of Euler [21] and Lagrange [51].

In the framework of the controllability of ideal fluids, lots of studies have been devoted to the Eulerian description since the first results of Coron [16].

Recently, O. Glass and T. Horsin [32] have extended the notion of controllability to the Lagrangian description of two-dimensional perfect fluids;

the case of three-dimensionnal perfect fluids has also been studied in [33]. Previously, some toy models were investigated in [39] and [40].

In Sections 3.1–3.6, we describe the results obtained by O. Glass and the second author and we present some work in progress with O. Glass, O. Kavian and G. Legendre.

### 3.1. The Lagrangian controllability

Let us conserve the notation in Section 2 and let us consider the Euler equations

$$u_t + (u \cdot \nabla)u + \nabla p = 0 \quad \text{in } Q_T, \quad (3.1)$$

$$\nabla \cdot u = 0 \quad \text{in } Q_T, \quad (3.2)$$

$$u|_{t=0} = u_0 \quad \text{in } \Omega. \quad (3.3)$$

Concerning the boundary conditions, we impose :

$$u \cdot n = 0 \quad \text{on } (\partial\Omega \setminus \Gamma) \times (0, T). \quad (3.4)$$

Nothing is said on what happens on  $\Gamma \times (0, T)$ , the part of the lateral boundary where one is assumed to act on the fluid.

Let  $\gamma_0$  and  $\gamma_1$  be two smooth Jordan curves in  $\Omega$ , i.e., two closed curves smoothly diffeomorphic to  $\mathbb{S}^1$ .

**Definition 3.1.** Let  $T > 0$  be a given time. We will say that the exact Lagrangian controllability of (3.1)-(3.4) between  $\gamma_0$  and  $\gamma_1$  holds at time  $T$  if, given a regular initial data  $u_0$  satisfying

$$\nabla \cdot u_0 = 0 \quad \text{in } \Omega, \quad (3.5)$$

$$u_0 \cdot n = 0 \quad \text{on } \partial\Omega \setminus \Gamma, \quad (3.6)$$

there exists a solution  $(u, p)$  to (3.1)-(3.4) such that

$$\phi^u(t, 0, \gamma_0) \subset \Omega \quad \forall t \in [0, T], \quad (3.7)$$

$$\phi^u(T, 0, \gamma_0) = \gamma_1, \quad (3.8)$$

up to reparameterization.

In the above definition, for any given regular vector field  $X$ , we denote by  $\phi^X = \phi^X(s, t, x)$  the solution to

$$\frac{\partial \phi}{\partial s}(s, t, x) = X(s, \phi(s, t, x)), \quad \phi(s, s, x) = x,$$

i.e., the associated *Lagrangian coordinate*.

In the sequel, for any Jordan curve  $\gamma$ ,  $\text{int}(\gamma)$  denotes the bounded connected component of  ${}^c\gamma$ . Our assumptions on the  $\gamma_j$  allow to consider the volume of  $\text{int}(\gamma_j)$ , which will be denoted  $|\text{int}(\gamma_j)|$ .

Due to the incompressibility condition (3.2), in order to have exact Lagrangian controllability between  $\gamma_0$  and  $\gamma_1$ , it is necessary to have

$$|\text{int}(\gamma_0)| = |\text{int}(\gamma_1)|.$$

Recall that, if one introduces  $w := \nabla \times u$ , then  $w$  satisfies

$$w_t + u \cdot \nabla w = 0, \tag{3.9}$$

that is,  $w$  is moved by the trajectories of  $\phi^u$ . This enabled O. Glass and T. Horsin in [32] to give counter-examples to the exact Lagrangian controllability that do not respect the condition (3.7). In fact, one can omit or relax (3.7), but this may imply that the controlled part of the fluid is allowed to leave  $\Omega$  which, concerning possible applications to moving pollutants, would not be admissible.

O. Glass and T. Horsin were thus led to give another definition:

**Definition 3.2.** We will say that the approximate Lagrangian controllability of (3.1)-(3.4) holds between  $\gamma_0$  and  $\gamma_1$  at time  $T$  and in norm  $C^{k,\alpha}$  if, for any given  $u_0$  as above and any  $\varepsilon > 0$ , there exists a solution  $(u, p)$  to (3.1)-(3.4) such that (3.7) holds and, moreover,

$$\|\phi^u(T, 0, \gamma_0) - \gamma_1\|_{C^{k,\alpha}(\mathbb{S}^1)} \leq \varepsilon, \tag{3.10}$$

up to reparameterization.

### 3.2. The main result in dimension 2

What has been proven in [32] is the following:

**Theorem 3.3.** *Assume that  $\gamma_0$  and  $\gamma_1$  are two Jordan curves that are homotopic in  $\Omega$ . Then, for any  $T > 0$ , any integer  $k \geq 1$  and any  $\alpha \in (0, 1)$ , the approximate Lagrangian controllability property between  $\gamma_0$  and  $\gamma_1$  holds at time  $T$  in norm  $C^{k,\alpha}$ .*

This result is sharp in the sense that some counter-examples can be exhibited if one does not relax the condition (3.8).

*Remark 3.4.* These counter-examples, based on the fact that the vorticity of  $u$  cannot be changed along the characteristics of  $u$  that do not leave  $\Omega$ ,

show that any attempt to perform a Lagrangian and Eulerian controllability simultaneously is impossible. In practice, this prevents from mixing the concepts and strategies in this and the previous Section. If one relaxes the condition (3.7), the work of Coron [16] allows to mix the Eulerian and Lagrangian controllability viewpoints, provided some control constraints are imposed to respect Kelvin's law; but, as noticed above, it seems that it is crucial for applications to keep (3.7).  $\square$

The main steps of the proof of Theorem 3.3 are the following:

- (1) First, to prove this result in the case  $u_0 = 0$ .
- (2) Then, to perform a rescaling argument, combined to the so-called "return method" introduced by Coron [16], in order to handle non-zero initial data.

The first step is in fact proven by using potential flows, while the proof of the second one relies on a formulation of the Euler equation in terms of the vorticity  $\omega$ , see [45].

### 3.3. The main result in dimension 3

In dimension 3, Glass and Horsin partially extended the result of dimension 2. This is not obvious: on one hand, some technical points used in the two-dimensional case are not known to be true whereas, on the other hand, blow-up may occur for the Euler equation in the three-dimensional case.

In dimension 3,  $\gamma_0$  and  $\gamma_1$  are now taken to be smoothly diffeomorphic to  $\mathbb{S}^2$ , that is, Jordan surfaces. What is proven in [33] is the following:

**Theorem 3.5.** *Let  $\alpha \in (0, 1)$  and  $k \geq 1$  be given. Consider a function  $u_0 \in C^{k,\alpha}(\bar{\Omega}; \mathbb{R}^3)$  satisfying (3.5)-(3.6) and two contractible  $C^\infty$  embeddings of  $\mathbb{S}^2$  in  $\Omega$ , denoted  $\gamma_0$  and  $\gamma_1$ . Then, for any  $\varepsilon > 0$ , there exist  $T > 0$  and a solution  $(u, p)$  to (3.1)-(3.4) in  $Q_T$  such that one has (3.7) and*

$$\|\phi^u(T, 0, \gamma_0) - \gamma_1\|_{C^{k,\alpha}(\mathbb{S}^2)} \leq \varepsilon$$

(up to reparameterization).

The result is again sharp and similar counter-examples to those in dimension 2 can be given.

Notice that, in both dimensions 2 and 3, the solution  $(u, p)$  that ascertains the result is smooth. Thus, from classical flow theorems, we have that  $\phi^u(T, 0, \cdot)$  is a diffeomorphism and  $\phi^u(T, 0, \cdot)$  maps approximately  $\text{int}(\gamma_0)$  into  $\text{int}(\gamma_1)$ .

In accordance with (3.9), it becomes clear that one cannot prescribe (even approximatively)  $\phi^u(T, 0, \gamma_0)$  and  $u(\cdot, T)$ , that is, it is not possible to perform Lagrangian and Eulerian controllability at the same time.

### 3.4. A cornerstone of the proofs

As already mentioned, one of the main steps in the proofs in dimensions 2 and 3 is the case  $u_0 = 0$ , where potential flows are used.

This means that we look for a solution  $(u, p)$  of the Euler equation with  $u = \nabla\psi$ , where  $\psi$  is a time-dependent harmonic map and

$$p = -u_t - |\nabla\psi|^2.$$

Accordingly, when considering smooth solutions to the Euler equations, if one wants to prescribe the motion of  $\gamma_0$ , it is enough to prescribe the normal velocity of  $\gamma_0$ .

Assume that there exists a  $C^\infty$  vector field  $X$  with compact support such that  $\nabla \cdot X = 0$ ,

$$\phi^X(t, 0, \gamma_0) \subset \Omega \quad \forall t \in [0, T]$$

and

$$\phi^X(T, 0, \gamma_0) = \gamma_1.$$

Then, in order to achieve the exact Lagrangian controllability property between  $\gamma_0$  and  $\gamma_1$  at time  $T$ , it is enough to construct a map

$$\psi : \overline{Q_T} \mapsto \mathbb{R},$$

such that

$$\Delta_x \psi = 0 \quad \forall t \in [0, T], \quad (3.11)$$

$$\nabla_x \psi \cdot \nu = X \cdot \nu \quad \text{on } \phi^{\nabla_x \psi}(t, 0, \gamma_0) \quad \forall t \in [0, T], \quad (3.12)$$

$$\nabla_x \psi \cdot n = 0 \quad \text{on } \partial\Omega \setminus \Gamma \quad \forall t \in [0, T], \quad (3.13)$$

$$\int_{\Gamma} \nabla_x \psi \cdot n \, d\sigma = 0 \quad \forall t \in [0, T], \quad (3.14)$$

where  $\nu$  denotes the unit outwards normal to  $\phi^{\nabla_x \psi}(t, 0, \gamma_0)$ .

This problem is ill-posed in general. In order to palliate this major difficulty, one may try to relax (3.12) and prove that, for any  $\varepsilon > 0$  there exists  $\psi$  such that (3.11), (3.13) and (3.14) hold, together with

$$\|\nabla_x \psi \cdot \nu - X \cdot \nu\| \leq \varepsilon \quad \text{on } \phi^{\nabla_x \psi}(t, 0, \gamma_0) \quad \forall t \in [0, T] \quad (3.15)$$

in an appropriate norm.

This is in fact doable through a compactness argument in time and the use of the famous *Runge's approximation theorem* and leads to the aforementioned results.

Thus, the proof relies on the existence of the vector field  $X$ . To this purpose, the following is established in [32] and [33]:

**Theorem 3.6.** *Under the hypotheses made on  $\gamma_0$  and  $\gamma_1$ , there exists  $X \in C_0^\infty(\Omega \times (0, T); \mathbb{R}^3)$  such that*

$$\nabla_x \cdot X = 0 \quad \forall t \in (0, T)$$

and

$$\phi^X(T, 0, \gamma_0) = \gamma_1.$$

The proof is explicit (but intricate) in dimension 2, whereas it relies on a result by A.B. Krygin [48] in dimension 3 (nevertheless, explicit but intricate constructions can also be performed in this case).

### 3.5. Towards numerics

This last section describes the starting point of an ongoing work with O. Glass, O. Kavian and G. Legendre concerning the effectiveness of Lagrangian controllability by performing numerical simulations.

Though instabilities occur at many steps of the numerics, the key points are an explicit construction of  $X$  satisfying Theorem 3.6 and an explicit construction of  $\psi$  satisfying (3.11), (3.13), (3.14) and (3.15).

The numerical construction of  $X$  is for the moment being a major difficulty which should be performed by using image processing, while the numerical construction of  $\psi$  can be achieved the following way.

We skip the dependence with respect to time in order to simplify the exposition and we assume that  $\Gamma$  is a connected component of  $\partial\Omega$  (this assumption may be released). In the sequel,  $\gamma$  will denote a Jordan curve or surface depending on the dimension and the associated outwards normal vector will be denoted again by  $\nu$ .

Let us introduce the space

$$H_m^{-1/2}(\Gamma) := \{v \in H^{-1/2}(\Gamma) : \langle v, 1 \rangle = 0, \quad v = 0 \text{ on } \partial\Omega \setminus \gamma\}.$$

Similarly, we can consider the space  $H_m^{-1/2}(\gamma)$ .

We consider the following mapping

$$\begin{aligned} \Lambda : H_m^{-1/2}(\Gamma) &\mapsto H_m^{-1/2}(\gamma) \\ v &\mapsto \nabla\psi \cdot \nu, \end{aligned}$$

where  $\psi$  satisfies

$$\begin{aligned} \Delta\psi &= 0, \quad x \in \Omega \\ \nabla\psi \cdot n &= v, \quad x \in \partial\Omega. \end{aligned}$$

Then, it can be proven that  $\Lambda$  has a dense image. Moreover, by means of the Fenchel-Rockefeller duality approach, given a target  $w \in H_m^{-1/2}(\gamma)$ , it is possible to find  $v \in H_m^{-1/2}(\Gamma)$  of minimal norm such that

$$\|\Lambda v - w\|_{-1/2,\gamma} \leq \varepsilon.$$

### 3.6. Extension to other models

In a work in progress, the second author and O. Glass have been able to extend Theorems 3.3 and 3.5 to the quasi-static Stokes equations

$$\begin{aligned} -\Delta u + \nabla p &= 0, \quad (x, t) \in \Omega \times (0, T) \\ \nabla \cdot u &= 0, \quad (x, t) \in \Omega \times (0, T) \\ u &= 0, \quad (x, t) \in (\partial\Omega \setminus \Gamma) \times (0, T) \\ \int_{\Gamma} u \cdot n \, d\sigma &= 0 \quad \forall t \in [0, T]. \end{aligned}$$

This model can be viewed as a good approximation of the Navier-Stokes equations in the situation of a very low Reynolds number and has been used in the framework of controllability in [55].

## 4. Vortex control of instationary channel flows using translation invariant cost functionals

Apart from solving controllability problems, there are other ways to control the behavior of a fluid. A very appropriate strategy is optimal control. This relies on the introduction of a cost functional (that depends on the

control and the state) and a family of constraints and the search of a control-state pair that minimizes the cost in the associated admissible set.

A particular and very important case is found when we investigate geometric vortex reduction in a flow.

The quantification of a “vortex” is still an issue that is not completely settled. Accordingly, we deal in this Section with the choice of an appropriate cost functional for vortex minimization in a flow field governed by the time-dependent Navier-Stokes equations. The controls are the parameters describing the shape of the domain.

A systematic study has been performed in [44] of the optimal shapes corresponding to the minimization of the three cost functionals

$$\begin{aligned} J_1(u) &= \frac{1}{2} \int_0^T \int_{\Omega} |u(x, t) - u_d(x, t)|^2 dx dt, \\ J_2(u) &= \frac{1}{2} \int_0^T \int_{\Omega} |\operatorname{curl} u(x, t)|^2 dx dt, \\ J_3(u) &= \int_0^T \int_{\Omega} g_3(\det \nabla u(x, t)) dx dt \end{aligned} \tag{4.1}$$

for vortex reduction in a flow field governed by stationary incompressible Navier-Stokes equations. Here,  $u_d$  denotes a given desired flow field without vortices and  $g_3 \in C^2(\mathbb{R})$  is a regularization of the function  $x \mapsto \max(0, x)$  [44]. Striking differences were found for the optimal shapes corresponding to the minimization of the previous functionals.

In the current work, we extend this study to flow fields governed by the instationary incompressible Navier-Stokes equations. A comparison is made on two particular problems. They consist of the minimization of vortices in instationary flows in a channel with a bump and a channel with an obstacle, respectively. For the purpose of minimization, a gradient type method is used. It relies on the characterization of the shape gradients for the three functionals in (4.1).

## 4.1. Setting of the problem

### 4.1.1. The state equation

Let  $\Omega \subset \mathbb{R}^2$  be a bounded domain with a piecewise regular boundary  $\partial\Omega$ . The state equation for the flow is the non-stationary Navier-Stokes system

$$\begin{aligned}
 u_t - \nu\Delta u + (u \cdot \nabla)u + \nabla p &= f, & (x, t) \in Q_T, \\
 \nabla \cdot u &= 0, & (x, t) \in Q_T, \\
 u &= g, & (x, t) \in \Gamma_{in} \times (0, T), \\
 u &= 0, & (x, t) \in (\Gamma_w \cup \Gamma_f) \times (0, T), \\
 \sigma(u, p) \cdot n &= 0, & (x, t) \in \Gamma_N \times (0, T), \quad \Gamma_N := \Gamma_{out}, \\
 u(x, 0) &= u_0(x), & x \in \Omega.
 \end{aligned} \tag{4.2}$$

As before,  $u$ ,  $p$  and  $\nu = 1/\text{Re} > 0$  are the velocity, the pressure and the kinematic viscosity of the fluid and  $\text{Re}$  is the Reynolds number of the flow;  $u_0$  is the initial velocity field and  $f$  is the density of external forces. We consider the problems described in Figure 4.1. In both problems,  $\Gamma_f$  is used as a control boundary by means of which the shape of  $\Omega$  is governed.

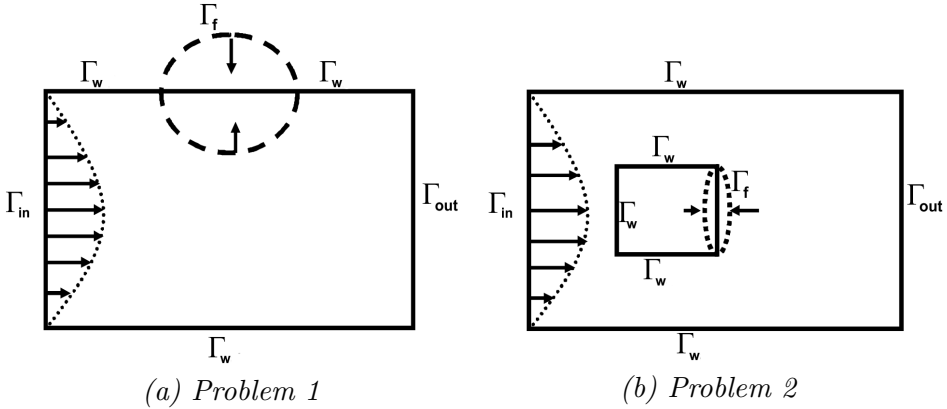


FIGURE 4.1. The domains for the test problems

### 4.1.2. The optimization problems

Our goal is to find the optimal  $\Gamma_f$  by minimizing the cost functionals, which depend on  $(\Omega, u)$ . Let  $\Gamma_f$  be described as a graph associated to the

curve  $\alpha: [a, b] \mapsto \mathbb{R}$ . This graph is given by

$$\Gamma_f(\alpha) = \{ (x_1, x_2) : x_1 \in [a, b], x_2 = \alpha(x_1) \}$$

for Problem 1 and

$$\Gamma_f(\alpha) = \{ (x_1, x_2) : x_1 = \alpha(x_2), x_2 \in [d, e] \}$$

for Problem 2, where  $a, b, d$ , and  $e$  are given constants. As a consequence, the admissible family of curves defining  $\Gamma_f(\alpha)$  for Problem 1 can be defined as follows:

$$\mathcal{U}_{ad} = \{ \alpha \in C^{0,1}([a, b]) : 0 < \alpha_{min} \leq \alpha(x_1) \leq \alpha_{max}, \\ \alpha(a) = \alpha_0, \alpha(b) = \alpha_1, |\alpha'| \leq L_1 \text{ a.e in } (a, b) \}.$$

In a similar way, we can define  $\mathcal{U}_{ad}$  for Problem 2.

The optimization problem can be written in the following form:

$$\begin{aligned} \text{Find } (\alpha^*, u^*, p^*) \in \mathcal{G} \text{ such that} \\ J(\Omega(\alpha^*), u(\alpha^*)) \leq J(\Omega(\alpha), u(\alpha)) \text{ for all } (\alpha, u, p) \in \mathcal{G}, \end{aligned} \tag{4.3}$$

where

$$\mathcal{G} := \{ (\alpha, u, p) : \alpha \in \mathcal{U}_{ad}, (u, p) \text{ is a weak solution to (4.2)} \}.$$

## 4.2. Sensitivity analysis

In this Section we discuss the necessary optimality conditions for (4.3).

More precisely, let  $D \subset \mathbb{R}^2$  be a fixed bounded  $C^{1,1}$  domain such that  $\bar{\Omega} \subset D$ . An admissible perturbation of the reference domain  $\Omega$  is described by a deformation field

$$h \in \mathcal{T}_{ad} := \{ h \in C^{1,1}(\bar{D}) : h|_{\partial D} = 0, h|_{\partial\Omega \setminus \Gamma_f} = 0 \}$$

and the family of  $C^{1,1}$  diffeomorphisms  $T_s : D \mapsto D$

$$T_s = \text{Id.} + sh, \quad |s| < \tilde{\tau}$$

for some sufficiently small  $\tilde{\tau}$ . Defining the perturbed domains  $\Omega_s = T_s(\Omega)$  and the perturbed manifolds  $\Gamma_s = T_s(\partial\Omega)$ , the Eulerian derivative of  $J$  at  $\Omega$  in the direction  $h$  is defined as

$$dJ(u, \Omega)h := \lim_{s \rightarrow 0^+} \frac{J(u_s, \Omega_s) - J(u, \Omega)}{s},$$

where the  $(u_s, p_s)$  satisfy

$$\begin{aligned} & (u_{s,t}, \psi_s)_{Q_s} + \nu(\nabla u_s, \nabla \psi_s)_{Q_s} + ((u_s \cdot \nabla)u_s, \psi_s)_{Q_s} - (p_s, \nabla \cdot \psi_s)_{Q_s} \\ & - (f_s, \psi_s)_{Q_s} - (\nabla \cdot u_s, \xi_s)_{Q_s} + (u_s(\cdot, 0) - u_{0,s}, \psi_s(\cdot, 0))_{\Omega_s} = 0 \end{aligned} \quad (4.4)$$

with  $(\psi_s, \xi_s) \in X_s$ ,  $Q_s = \Omega_s \times (0, T)$ ,  $u_{0,s} = u_0|_{\Omega_s}$ ,  $f_s = f|_{\Omega_s}$  and

$$X_s := L^2(I; H_0^1(\Omega_s)) \times L^2(I; L_0^2(\Omega_s)).$$

In (4.4),  $(\cdot, \cdot)_{Q_s}$  and  $(\cdot, \cdot)_{\Omega_s}$  respectively denote the usual scalar products in  $L^2(Q_s)$  and  $L^2(\Omega_s)$ .

Observe that, at  $s = 0$ , (4.4) becomes

$$\begin{aligned} & (u_t, \psi)_Q + \nu(\nabla u, \nabla \psi)_Q + ((u \cdot \nabla)u, \psi)_Q - (p, \nabla \cdot \psi)_Q - (f, \psi)_Q \\ & - (\nabla \cdot u, \xi)_Q + (u(\cdot, 0) - u_0, \psi(\cdot, 0))_{\Omega} = 0 \end{aligned} \quad (4.5)$$

which is the weak form of (4.2).

**Theorem 4.1.** *Under appropriate assumptions (see [43] for more details), one can show that the Eulerian derivatives of the cost functionals  $J_\ell$  exist for  $\ell = 1, 2, 3$  and are given by*

$$dJ_\ell(u, \Omega)h = \int_{\Gamma_f} \left( \int_0^T G_\ell(u(x, t), \lambda(x, t)) dt \right) h(x) \cdot n(x) d\Gamma,$$

where

$$\begin{aligned} G_1 & := \left[ \nu \frac{\partial u}{\partial n} \frac{\partial \lambda}{\partial n} + \frac{1}{2}(u - u_d)^2 \right] \\ G_2 & := \left[ \nu \frac{\partial u}{\partial n} \frac{\partial \lambda}{\partial n} + \frac{1}{2}|\nabla \times u|^2 - (\nabla \times u)\tau \cdot \frac{\partial u}{\partial n} \right] \\ G_3 & := \left[ \nu \frac{\partial u}{\partial n} \frac{\partial \lambda}{\partial n} + g_3(\det \nabla u) - P(u) \frac{\partial u}{\partial n} \right] \end{aligned}$$

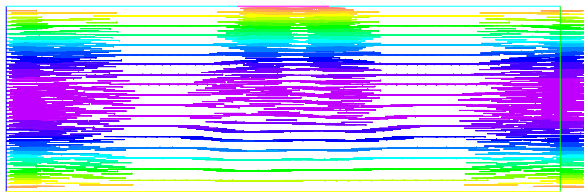
and  $(\lambda, q)$  satisfies

$$\begin{aligned} & (\psi_t, \lambda)_Q + \nu(\nabla \psi, \nabla \lambda)_Q + ((\psi \cdot \nabla)\mathbf{u} + (u \cdot \nabla)\psi, \lambda)_Q - (\xi, \nabla \cdot \lambda)_Q \\ & + (\nabla \cdot \psi, q)_Q + (\psi(\cdot, 0), \lambda(\cdot, 0))_{\Omega} = A_i(u, \psi) \end{aligned} \quad (4.6)$$

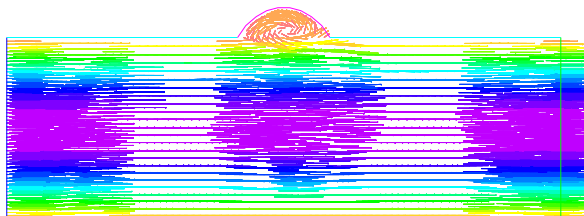
with  $A_1(u, \psi) = (u - u_d, \psi)_Q$ ,  $A_2(u, \psi) = (\nabla \times u, \nabla \times \psi)_Q$ ,  $A_3(u, \psi) = (g'_3(\det \nabla u), \det \nabla \psi)_Q$ .

If  $\Gamma_f$  is parameterized using Bézier curves so that any point  $x(s)$  on  $\Gamma_f$  is given by

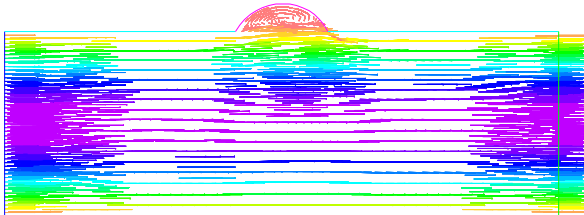
$$x(s) = \sum_{j=0}^n b_j B_j^{(n)}(s), \quad s \in [0, 1], \quad B_i^{(n)}(s) = \binom{n}{i} s^i (1-s)^{n-i}$$



(a) Initial flow,  $Re = 50$ , min. and max. speed: 0. and 2.50.



(b) Optimal shape for  $J_1$  and  $J_3$ , min. and max. speed: 0. and 5.00.



(c) Optimal shape for  $J_2$ , min. and max. speed: 0. and 5.00.

FIGURE 4.2. Initial and optimal domains.

and  $\{b_j\}_{j=0}^n$  is a set of  $n + 1$  control points, then one can show that the shape derivative of  $J_\ell$  can be expressed in the form

$$dJ_\ell(u, \Omega)h = \sum_{j=0}^n \left( \begin{array}{c} \sum_{i=0}^n a_{i,j}^\ell b_{i,2} \\ - \sum_{i=0}^n a_{i,j}^\ell b_{i,1} \end{array} \right)^T \begin{pmatrix} z_{j,1} \\ z_{j,2} \end{pmatrix},$$

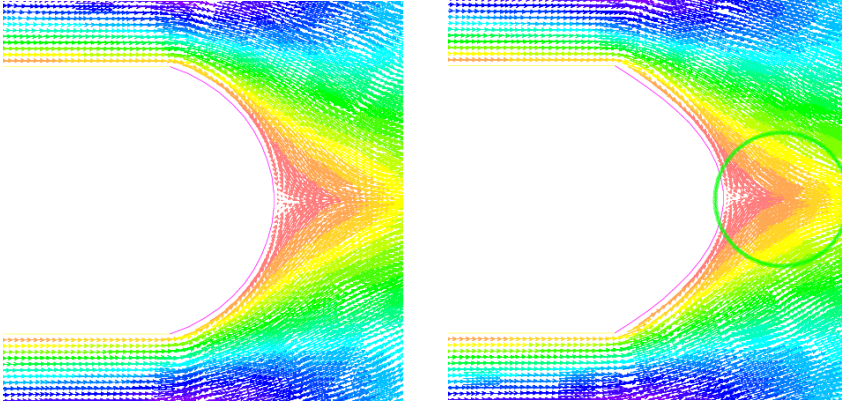
where

$$a_{i,j}^\ell = \int_0^1 \left[ \int_0^T G_\ell(u(x(s), t), p(x(s), t)) dt \right] B_j^{(n)}(s) B_i'^{(n)}(s) ds,$$

and

$$h(x(s)) = \sum_{j=0}^n z_j B_j^{(n)}(s).$$

Therefore, the choice  $z_{j,1} = -\sum_{i=0}^n a_{i,j}^\ell b_{i,2}$  and  $z_{j,2} = \sum_{i=0}^n a_{i,j}^\ell b_{i,1}$  provides a descent direction for the cost functionals  $J_\ell$ .



(a) The initial field.

(b) The flow in  $\Omega_f$ .

FIGURE 4.3. Cost function  $J_1$ . The velocity fields for the initial and optimal geometry.

### 4.3. Numerical algorithm and examples

Next, we present the algorithm that we have used to solve the shape optimization problems. We denote by  $\Omega_0$ ,  $\Omega_f$  the initial and final shapes, respectively.

The domain  $\Omega$  is deformed according to Algorithm 1.

#### 4.3.1. Test case 1: flow in a channel with a bump

The dimensions of the channel are as follows:  $-3 < x_1 < 3$  and  $-1 < x_2 < 1$  with a bump  $\Gamma_f$  on the upper wall extending from  $x_1 = -0.5$  to  $x_1 = 0.5$ .

---

**Algorithm 1** The boundary variation algorithm

---

1. Choose the initial shape  $\Omega_0$  and control points  $b^0 = (b_0, b_1, \dots, b_n)$ ,  $b_j \in \mathbb{R}^2$ .
2. Compute the state system (4.5) and the adjoint system (4.6).
3. Compute the entries of the matrix  $A = (a_{i,j})$ .
4. Compute the descent direction  $z$  for the control points  $b$  via

$$z_{x_1} = -A^T b_{x_2} \quad z_{x_2} = A^T b_{x_1},$$

where  $z_{x_1} = \{z_{j,1}\}_{j=0}^n$ ,  $z_{x_2} = \{z_{j,2}\}_{j=0}^n$ ,  $b_{x_1} = \{b_{j,1}\}_{j=0}^n$  and  $b_{x_2} = \{b_{j,2}\}_{j=0}^n$ .

4. Update the control points via  $b^{k+1} = b^k + \tau z^k$ ; the corresponding control boundary and domain are given by  $x_\tau(s)^{k+1} = \sum_{j=0}^n (b_j^k + \tau z_j^k) B_j^{(n)}(s)$  and  $\Omega_{k+1} = \Omega_{[b^k + \tau z^k]}$ , respectively. Here,  $\tau$  is a positive number.
- 

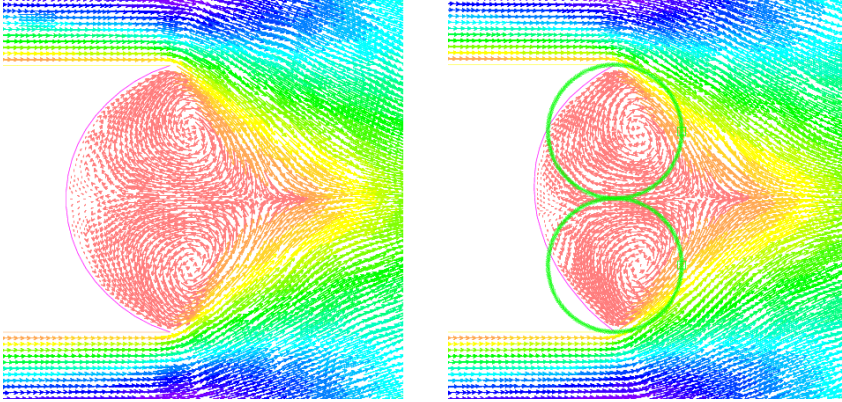
The parameters defining  $\mathcal{U}_{ad}$  are  $\alpha_0 = 1$ ,  $\alpha_1 = 1$ ,  $L_1 = 1$ ,  $\alpha_{min}(x_1) = 0.5$  and  $\alpha_{max}(x_1) = 1.5$ .

The physical parameters are chosen as follows:  $Re = 50$ ,  $g = (5(1 - x_2^2), 0)$  and  $f = 0$ ;  $\Gamma_f$  is constructed using a Bézier polynomial of degree 3. In other words, we have four control points for the optimization, of which the two end points are fixed.

The Taylor-Hood elements are used for the approximation of the velocity and pressure.

At each time step, the discretized equations are solved by a direct method based on the  $LU$  factorization of the matrix. We fix  $T = 1$  and set  $\Delta t = 0.1$ . The uncontrolled velocity field obtained after 10 time steps possesses a vortex in the bump region of the computational domain (Figure 4.2 (a)). Our goal is reduction/minimization by means of  $\Gamma_f$ ;  $u_d$  is chosen as  $u_d = (5(1 - x_2^2), 0)$ .

Algorithm 1 is initialized with  $\Omega_0$ , depicted in Figure 4.2 (a). The value of  $J_1$  at  $\Omega_0$  is 0.2872. Algorithm 1 is stopped as soon as the Euclidean norm  $|b^{k+1} - b^k|_2 < 10^{-4}$ . As expected, after 9 iterates, we obtain an axis-parallel flow field (see Figure 4.2 (b)). The value of  $J_1$  at  $\Omega_f$  is  $5.89 \times 10^{-7}$ .



(a) The initial field.

 (b) The flow in  $\Omega_f$ .

 FIGURE 4.4. Cost function  $J_2$ . The velocity fields for the initial and optimal geometry.

Next, we turn our attention to the the minimization of  $J_2$ . A plot of cost vs. iterates for  $J_2$  during the minimization process according to  $J_1$  suggested choosing a different domain  $\Omega$  for the initialization of Algorithm 1. To this end, we initialize Algorithm 1 with the set  $\Omega_0$  depicted in Figure 4.2 (b). The flow field computed at this domain is axis-parallel and the value of  $J_2$  is found to be 200.

After 10 iterates, the value of  $J_2$  at  $\Omega_f$  (Figure 4.2 (c)) is 197.90, which gives a relative reduction of 1.05% the initial cost. From Figure 4.2 (c), we see that although we have reduced the value of  $J_2$ , a vortex is created. This result can be explained from the physical viewpoint using the conservation of energy principle, see [44] for details.

Next, we minimize  $J_3$ . Algorithm 1 is initialized with  $\Omega_0$  depicted in Figure 4.2 (a). Similar results as in the case of  $J_1$  are obtained. We note that the optimal geometry obtained when using  $J_1$  depends on the definition of  $u_d$ .

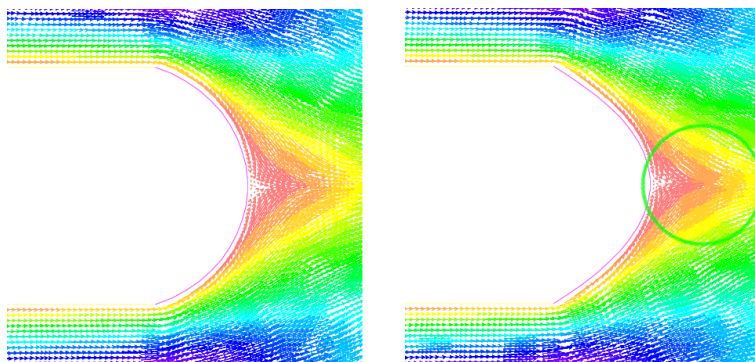
These results indicate that the frequently used cost functional  $J_2$  does not seem to be a good candidate for vortex reduction in instationary flows in channels. In fact,  $J_3$  should be preferred to  $J_1$  and  $J_2$ .

### 4.3.2. Test case 2: flow in a channel with an obstacle

The parameters defining  $\mathcal{U}_{ad}$  are  $\alpha_0 = 0.2$ ,  $\alpha_1 = 0.2$ ,  $L_2 = 1$ ,  $\alpha_{min}(x_2) = -0.05$  and  $\alpha_{max}(x_2) = 0.45$ .  $\Gamma_f$  is constructed using a Bézier polynomial of degree five, i.e., we have 6 control points for the optimization, of which the two end points are fixed. The resulting computational domains are then discretized by triangular elements generated by a bi-dimensional anisotropic mesh generator.

We set  $g = (2(0.25 - x_2^2), 0)$ ,  $Re=120$ ,  $f = 0$ ,  $T = 1$  and  $\Delta t = 0.1$ .

Due to the fact that the cost functionals are non-convex, the initialization of Algorithm 1 can be important. This information is obtained after a direct numerical simulation on the three different geometrical configurations [44]. The optimization with  $J_1$  is initialized with  $\Omega_0$  shown in Figure 4.3 (a) and  $u_d = (2(0.25 - x_2^2), 0)$ .



(a) The initial field.

(b) The flow in  $\Omega_f$ .

FIGURE 4.5. Cost function  $J_3$ . The velocity fields for the initial and optimal geometry.

In Figure 4.3 (b), we show  $\Omega_f$  and the flow field obtained after 12 iterates. The value of  $J_1$  at  $\Omega_0$  is found to be 0.0447 while the value at  $\Omega_f$  is 0.0440. The cost has been reduced by 1.66% with respect to the initial value. A zoom into the region marked by a circle in Figure 4.3(b) indicates no visual presence of vortices in the final flow field.

Next, we optimize with  $J_2$ . Here, Algorithm 1 is initialized with  $\Omega_0$  depicted in Figure 4.4 (a). In Figure 4.4 (b), we show the domain  $\Omega_f$  obtained after 15 iterates. The value of  $J_2$  at  $\Omega_0$  is found to be 8.9764, while that at  $\Omega_f$  is 8.9330. This gives a relative reduction of 0.48% in the value of the cost. However, small vortices are still visible in the region marked by two bold circles in Figure 4.4 (b).

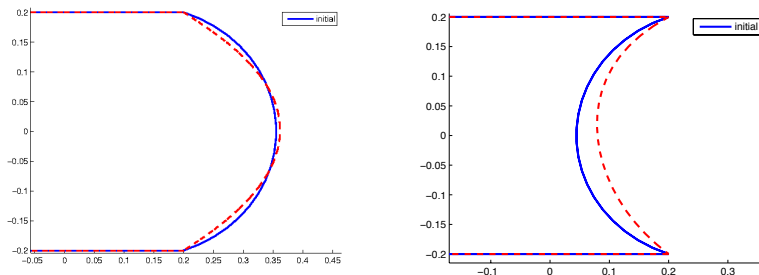
Next we optimize with  $J_3$ . Algorithm 1 is initialized with  $\Omega_0$  and the flow is depicted in Figure 4.5 (a).

$J_3$  is found to be 0.7841 and 0.7763 at  $\Omega_0$  and  $\Omega_f$  (Figure 4.5 (b)), respectively. This gives a relative reduction of 1% in the value of the cost after 9 iterates. A further zoom of the final flow field in the region marked with a circle in Figure 4.5 (b) indicates no visual presence of vortices in the flow field.

The location of the initial and final  $\Gamma_f$  are depicted in Figure 4.6.

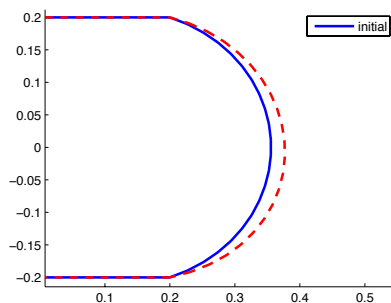
Considering the fact that  $J_1$  was computed with a good choice of  $u_d$ , we can summarize that  $J_3$  performs better than  $J_1$  and  $J_2$  as a means to reduce the vortex in the region behind the obstacle.

**Acknowledgements:** The first author was partially financed by DGI-Spain, Grant MTM2010-15992.



(a) Cost function  $J_1$ .

(b) Cost function  $J_2$ .



(c) Cost function  $J_3$ .

FIGURE 4.6. The initial and final profiles  $\Gamma_f$ .

## References

- [1] G. ALESSANDRINI, E. BERETTA, E. ROSSET & S. VESSELLA – “Optimal stability for inverse elliptic boundary value problems with unknown boundaries”, *Ann. Scuola Norm. Sup. Pisa Cl. Sci. (4)* **29** (2000), no. 4, p. 755–806.
- [2] C. ALVAREZ, C. CONCA, L. FRIZ, O. KAVIAN & J. H. ORTEGA – “Identification of immersed obstacles via boundary measurements”, *Inverse Problems* **21** (2005), no. 5, p. 1531–1552.
- [3] S. ANDRIEUX, A. BEN ABDA & M. JAOU – “On some inverse geometrical problems”, in *Partial differential equation methods in control*

- and shape analysis (Pisa)*, Lecture Notes in Pure and Appl. Math., vol. 188, Dekker, New York, 1997, p. 11–27.
- [4] K. J. ARROW, L. HURWICZ & H. UZAWA – *Studies in linear and non-linear programming*, With contributions by H. B. Chenery, S. M. Johnson, S. Karlin, T. Marschak, R. M. Solow. Stanford Mathematical Studies in the Social Sciences, vol. II, Stanford University Press, Stanford, Calif., 1958.
- [5] M. BADRA, F. CAUBET & M. DAMBRINE – “Detecting an obstacle immersed in a fluid by shape optimization methods”, *Math. Models Methods Appl. Sci.* **21** (2011), no. 10, p. 2069–2101.
- [6] J. A. BELLO, E. FERNÁNDEZ-CARA, J. LEMOINE & J. SIMON – “The differentiability of the drag with respect to the variations of a Lipschitz domain in a Navier-Stokes flow”, *SIAM J. Control Optim.* **35** (1997), no. 2, p. 626–640.
- [7] F. BEN BELGACEM & S. M. KABER – “On the Dirichlet boundary controllability of the one-dimensional heat equation: semi-analytical calculations and ill-posedness degree”, *Inverse Problems* **27** (2011), no. 5, p. 055012, 19.
- [8] F. BOYER, F. HUBERT & J. LE ROUSSEAU – “Uniform controllability properties for space/time-discretized parabolic equations”, *Numer. Math.* **118** (2011), no. 4, p. 601–661.
- [9] B. CANUTO & O. KAVIAN – “Determining coefficients in a class of heat equations via boundary measurements”, *SIAM J. Math. Anal.* **32** (2001), no. 5, p. 963–986 (electronic).
- [10] C. CARTEL, R. GLOWINSKI & J.-L. LIONS – “On exact and approximate boundary controllabilities for the heat equation: a numerical approach”, *J. Optim. Theory Appl.* **82** (1994), no. 3, p. 429–484.
- [11] A. BERMÚDEZ DE CASTRO – *Continuum thermomechanics*, Progress in Mathematical Physics, vol. 43, Birkhäuser Verlag, Basel, 2005.
- [12] N. CINDEA, E. FERNÁNDEZ-CARA & A. MÜNCH – “Numerical null controllability of the wave equation with a primal approach: convergence results”, *ESAIM: COCV (to appear, 2013)*, no. 3.
- [13] N. CINDEA, E. FERNÁNDEZ-CARA, A. MÜNCH & D. DE SOUZA – “On the numerical null controllability of the Stokes and Navier-Stokes systems”, *In preparation* (2013).

- [14] C. CONCA, E. L. SCHWINDT & T. TAKAHASHI – “On the identifiability of a rigid body moving in a stationary viscous fluid”, *Inverse Problems* **28** (2012), no. 1, p. 015005, 22.
- [15] J.-M. CORON – “On the controllability of the 2-D incompressible Navier-Stokes equations with the Navier slip boundary conditions”, *ESAIM Contrôle Optim. Calc. Var.* **1** (1995/96), p. 35–75 (electronic).
- [16] ———, “On the controllability of 2-D incompressible perfect fluids”, *J. Math. Pures Appl. (9)* **75** (1996), no. 2, p. 155–188.
- [17] J.-M. CORON & A. V. FURSIKOV – “Global exact controllability of the 2D Navier-Stokes equations on a manifold without boundary”, *Russian J. Math. Phys.* **4** (1996), no. 4, p. 429–448.
- [18] A. DOUBOVA, E. FERNÁNDEZ-CARA, M. GONZÁLEZ-BURGOS & J. H. ORTEGA – “A geometric inverse problem for the Boussinesq system”, *Discrete Contin. Dyn. Syst. Ser. B* **6** (2006), no. 6, p. 1213–1238.
- [19] A. DOUBOVA, E. FERNÁNDEZ-CARA & J. H. ORTEGA – “On the identification of a single body immersed in a Navier-Stokes fluid”, *European J. Appl. Math.* **18** (2007), no. 1, p. 57–80.
- [20] S. ERVEDOZA & J. VALEIN – “On the observability of abstract time-discrete linear parabolic equations”, *Rev. Mat. Complut.* **23** (2010), no. 1, p. 163–190.
- [21] L. EULER – “General laws of the motion of fluids”, *Izv. Ross. Akad. Nauk Mekh. Zhidk. Gaza* (1999), no. 6, p. 26–54.
- [22] C. FABRE – “Uniqueness results for Stokes equations and their consequences in linear and nonlinear control problems”, *ESAIM Contrôle Optim. Calc. Var.* **1** (1995/96), p. 267–302 (electronic).
- [23] E. FERNÁNDEZ-CARA, S. GUERRERO, O. Y. IMANUVILOV & J.-P. PUEL – “Local exact controllability of the Navier-Stokes system”, *J. Math. Pures Appl. (9)* **83** (2004), no. 12, p. 1501–1542.
- [24] ———, “Some controllability results for the  $N$ -dimensional Navier-Stokes and Boussinesq systems with  $N - 1$  scalar controls”, *SIAM J. Control Optim.* **45** (2006), no. 1, p. 146–173 (electronic).

- [25] E. FERNÁNDEZ-CARA & A. MÜNCH – “Numerical null controllability of semi-linear 1-D heat equations: fixed point, least squares and Newton methods”, *Math. Control Relat. Fields* **2** (2012), no. 3, p. 217–246.
- [26] ———, “Strong convergent approximations of null controls for the 1D heat equation”, *SeMA Journal* **61** (2013), no. 1, p. 49–78.
- [27] A. FOWLER – *Mathematical geoscience*, Interdisciplinary Applied Mathematics, vol. 36, Springer, London, 2011.
- [28] A. V. FURSIKOV – “Exact controllability and feedback stabilization from a boundary for the Navier-Stokes equations”, in *Control of fluid flow*, Lecture Notes in Control and Inform. Sci., vol. 330, Springer, Berlin, 2006, p. 173–188.
- [29] A. V. FURSIKOV, M. GUNZBURGER, L. S. HOU & S. MANSERVISI – “Optimal control problems for the Navier-Stokes equations”, in *Lectures on applied mathematics (Munich, 1999)*, Springer, Berlin, 2000, p. 143–155.
- [30] A. V. FURSIKOV & O. Y. IMANUILOV – “Exact controllability of the Navier-Stokes and Boussinesq equations”, *Uspekhi Mat. Nauk* **54** (1999), no. 3(327), p. 93–146.
- [31] A. V. FURSIKOV & O. Y. IMANUILOV – *Controllability of evolution equations*, Lecture Notes Series, vol. 34, Seoul National University Research Institute of Mathematics Global Analysis Research Center, Seoul, 1996.
- [32] O. GLASS & T. HORSIN – “Approximate Lagrangian controllability for the 2-D Euler equation. Application to the control of the shape of vortex patches”, *J. Math. Pures Appl. (9)* **93** (2010), no. 1, p. 61–90.
- [33] ———, “Prescribing the Motion of a Set of Particles in a Three-Dimensional Perfect Fluid”, *SIAM J. Control Optim.* **50** (2012), no. 5, p. 2726–2742.
- [34] R. GLOWINSKI – *Numerical methods for nonlinear variational problems*, Scientific Computation, Springer-Verlag, Berlin, 2008, Reprint of the 1984 original.

- [35] R. GLOWINSKI, J.-L. LIONS & J. HE – *Exact and approximate controllability for distributed parameter systems*, Encyclopedia of Mathematics and its Applications, vol. 117, Cambridge University Press, Cambridge, 2008, A numerical approach.
- [36] M. GONZÁLEZ-BURGOS, S. GUERRERO & J.-P. PUEL – “Local exact controllability to the trajectories of the Boussinesq system via a fictitious control on the divergence equation”, *Commun. Pure Appl. Anal.* **8** (2009), no. 1, p. 311–333.
- [37] M. D. GUNZBURGER – *Perspectives in flow control and optimization*, Advances in Design and Control, vol. 5, Society for Industrial and Applied Mathematics (SIAM), Philadelphia, PA, 2003.
- [38] M. HINZE & K. KUNISCH – “Second order methods for optimal control of time-dependent fluid flow”, *SIAM J. Control Optim.* **40** (2001), no. 3, p. 925–946 (electronic).
- [39] T. HORSIN – “Application of the exact null controllability of the heat equation to moving sets”, *C. R. Math. Acad. Sci. Paris* **342** (2006), no. 11, p. 849–852.
- [40] ———, “Local exact Lagrangian controllability of the Burgers viscous equation”, *Ann. Inst. H. Poincaré Anal. Non Linéaire* **25** (2008), no. 2, p. 219–230.
- [41] O. Y. IMANUVILOV – “Remarks on exact controllability for the Navier-Stokes equations”, *ESAIM Control Optim. Calc. Var.* **6** (2001), p. 39–72 (electronic).
- [42] V. ISAKOV – *Inverse problems for partial differential equations*, second éd., Applied Mathematical Sciences, vol. 127, Springer, New York, 2006.
- [43] H. KASUMBA & K. KUNISCH – “On free surface PDE constrained shape optimization problems”, *Appl. Math. Comput.* **218** (2012), no. 23, p. 11429–11450.
- [44] ———, “Vortex control in channel flows using translational invariant cost functionals”, *Comput. Optim. Appl.* **52** (2012), no. 3, p. 691–717.
- [45] T. KATO – “On classical solutions of the two-dimensional nonstationary Euler equation”, *Arch. Rational Mech. Anal.* **25** (1967), p. 188–200.

- [46] S. KINDERMANN – “Convergence rates of the Hilbert uniqueness method via Tikhonov regularization”, *J. Optim. Theory Appl.* **103** (1999), no. 3, p. 657–673.
- [47] M. V. KLIBANOV & A. TIMONOV – *Carleman estimates for coefficient inverse problems and numerical applications*, Inverse and Ill-posed Problems Series, VSP, Utrecht, 2004.
- [48] A. B. KRYGIN – “Extension of diffeomorphisms that preserve volume”, *Funkcional. Anal. i Priložen.* **5** (1971), no. 2, p. 72–76.
- [49] K. KUNISCH & B. VEXLER – “Optimal vortex reduction for instationary flows based on translation invariant cost functionals”, *SIAM J. Control Optim.* **46** (2007), no. 4, p. 1368–1397.
- [50] S. LABBÉ & E. TRÉLAT – “Uniform controllability of semidiscrete approximations of parabolic control systems”, *Systems Control Lett.* **55** (2006), no. 7, p. 597–609.
- [51] J. L. LAGRANGE – *Oeuvres. Tome 14*, Gauthier-Villars (Paris), Hildesheim, 1967–1892, Publiées par les soins de J.-A. Serret [et G. Darboux] ; [Précédé d’une notice sur la vie et les ouvrages de J.-L. Lagrange, par M. Delambre].
- [52] S. MICU & E. ZUAZUA – “Regularity issues for the null-controllability of the linear 1-d heat equation”, *Systems Control Lett.* **60** (2011), no. 6, p. 406–413.
- [53] A. MÜNCH & E. ZUAZUA – “Numerical approximation of null controls for the heat equation: ill-posedness and remedies”, *Inverse Problems* **26** (2010), no. 8, p. 085018, 39.
- [54] A. A. SAMARSKII & P. N. VABISHCHEVICH – *Numerical methods for solving inverse problems of mathematical physics*, Inverse and Ill-posed Problems Series, Walter de Gruyter GmbH & Co. KG, Berlin, 2007.
- [55] J. SAN MARTÍN, T. TAKAHASHI & M. TUCSNAK – “A control theoretic approach to the swimming of microscopic organisms”, *Quart. Appl. Math.* **65** (2007), no. 3, p. 405–424.
- [56] W. YAN, Y. HE & Y. MA – “Shape reconstruction of an inverse boundary value problem of two-dimensional Navier-Stokes equations”, *Internat. J. Numer. Methods Fluids* **62** (2010), no. 6, p. 632–646.

E. FERNÁNDEZ-CARA, T. HORSIN & H. KASUMBA

ENRIQUE FERNÁNDEZ-CARA  
Dpto. EDAN  
University of Sevilla  
Aptdo. 1160, 41080 Sevilla  
SPAIN  
cara@us.es

THIERRY HORSIN  
IMath - Ingénierie Mathématique  
CNAM, 292, rue Saint Martin - case  
courrier 2D5000  
75141 Paris Cedex 03  
FRANCE  
thierry.horsin@cnam.fr

HENRY KASUMBA  
Radon Institute of Industrial and  
Applied Mathematics  
Austrian Academy of Sciences  
Altenbergstrasse 69 A-4040 Linz  
AUSTRIA  
henry.kasumba@oeaw.ac.at